

Ctr1 drives intestinal copper absorption and is essential for growth, iron metabolism, and neonatal cardiac function

Yasuhiro Nose,¹ Byung-Eun Kim,¹ and Dennis J. Thiele^{1,*}

¹Department of Pharmacology and Cancer Biology, Sarah W. Stedman Nutrition and Metabolism Center, Duke University Medical Center, Durham, North Carolina 27710

*Correspondence: dennis.thiele@duke.edu

Summary

The trace element copper (Cu) is a cofactor for biochemical functions ranging from energy generation to iron (Fe) acquisition, angiogenesis, and free radical detoxification. While Cu is essential for life, the molecules that mediate dietary Cu uptake have not been identified. Ctr1 is a homotrimeric protein, conserved from yeast to humans, that transports Cu across the plasma membrane with high affinity and specificity. Here we describe the generation of intestinal epithelial cell-specific Ctr1 knock-out mice. These mice exhibit striking neonatal defects in Cu accumulation in peripheral tissues, hepatic Fe overload, cardiac hypertrophy, and severe growth and viability defects. Consistent with an intestinal Cu absorption block, the growth and viability defects can be partially rescued by a single postnatal Cu administration, indicative of a critical neonatal metabolic requirement for Cu that is provided by intestinal Ctr1. These studies identify Ctr1 as the major factor driving intestinal Cu absorption in mammals.

Introduction

The ability of copper (Cu) to undergo changes in redox state has been harnessed by aerobic organisms to drive enzyme catalysis, signal transduction, and protein structure. Indeed, Cu is an essential nutrient for all eukaryotic organisms due to its function with enzymes that participate in a broad range of critical processes that include respiration, neuropeptide maturation, protection from oxidative stress, neurotransmitter biogenesis, pigmentation, angiogenesis, iron (Fe) absorption, connective tissue maturation, and a host of other key biological functions (Linder, 1991; Peña et al., 1999; Puig and Thiele, 2002). Consistent with the importance of these Cu-dependent processes, genetically programmed or dietarily induced Cu deficiency in mammals results in impaired motor function, reduced aortic elasticity, neutropenia, cardiac hypertrophy, anemia, severe cognitive disorders, growth defects, and other pathological states (Linder, 1991; Prohaska, 2000; Shim and Harris, 2003). In general, younger animals are more susceptible to Cu deficiency as compared to mature animals, but the precise mechanisms for this differential sensitivity are not well understood (Uauy et al., 1998; Prohaska and Brokate, 2002).

Currently much is known with respect to the proteins that carry out Cu homeostasis at the cellular level and their regulation (reviewed in Peña et al., 1999; Puig and Thiele, 2002). In organisms from yeast to humans, a conserved homotrimeric plasma membrane protein, Ctr1, mediates Cu import with high affinity and specificity (Lee et al., 2002a; Puig et al., 2002; Eisses et al., 2005). After import, Cu is targeted to proteins or organelles by specific Cu chaperone proteins that function in the delivery of Cu to mitochondrial cytochrome oxidase (via Cox17), to Cu,Zn superoxide dismutase (via CCS), and (via Atox1) to the cytosolic Cu binding domain of the P-type Cu-transporting ATPases, ATP7A or ATP7B, which deliver Cu to the lumen of a late secre-

tory compartment where it is loaded onto Cu-requiring proteins (Huffman and O'Halloran, 2001; Lutsenko and Petris, 2002; Luk et al., 2003). One such protein is hephaestin (Heph), a transmembrane copper-dependent ferroxidase that functions, in addition to ferroportin, to move iron (Fe) across the basolateral membrane of intestinal epithelial cells into the circulation. In mouse models, defects in hephaestin function underlie sex-linked anemia (Vulpe et al., 1999). In the bloodstream another multicopper ferroxidase, ceruloplasmin (Cp), oxidizes Fe(II) to Fe(III), thereby facilitating the loading of Fe(III) onto transferrin for delivery to peripheral organs via transferrin receptor-mediated endocytosis (Andrews, 2000; Hellman and Gitlin, 2002; Kaplan, 2002). Aceruloplasminemic patients or Cp knockout mice suffer from progressive Fe accumulation (Harris et al., 1995; Waggoner et al., 1999; Hellman and Gitlin, 2002). As such, Heph and Cp constitute critical biochemical links between Cu availability and normal Fe acquisition and distribution (Hellman and Gitlin, 2002; Fox, 2003). Cu is delivered across the basolateral membrane of intestinal epithelial cells via the trafficking of ATP7A to the basolateral membrane when Cu levels are elevated, providing a regulated means of moving Cu from the point of apical absorption to the site of exit for peripheral distribution (Llanos and Mercer, 2002). Patients harboring a nonfunctional ATP7A gene inherit Menkes kinky hair disease, a lethal childhood disease of Cu overload in intestinal epithelial cells and deficiency in the periphery (Lutsenko and Petris, 2002; Llanos and Mercer, 2002).

Previous studies suggest that Cu is absorbed in the small intestine via a carrier-mediated, saturable process (Linder, 1991). Furthermore, the efficiency of Cu uptake has been demonstrated to be modulated by dietary Cu status; when dietary Cu status is low, Cu is absorbed more efficiently than when Cu status is high (Turnlund, 1998). These studies suggest the presence of one or more specific molecules that carry out intestinal Cu absorption and the possibility that expression, activity, or

localization of these molecules may be regulated in response to Cu status. At present the identity of proteins that mediate intestinal epithelial Cu transport is unknown. While studies suggest that the broad spectrum metal transporter DMT1 transports Cu(I) into cultured polarized epithelial cells (Ferruzza et al., 2000; Arredondo et al., 2003), DMT1 has specificity for divalent metal ions (Gunshin et al., 1997).

Mammalian cell culture studies strongly support a role for Ctr1 in cellular Cu uptake (Lee et al., 2002a; Puig et al., 2002; Eisses et al., 2005). Ctr1 exhibits a K_m for Cu of $\sim 1 \mu\text{M}$, shows exquisite specificity for Cu, and transports Cu in an ATP-independent manner via conserved methionine residues located in the hydrophilic amino terminus and within the second of three transmembrane domains (Puig et al., 2002). Biochemical, genetic, and recent two-dimensional electron microscopy studies indicate that Ctr1 forms a pore for metal movement across membranes via the formation of a homotrimer (Lee et al., 2002a; Puig et al., 2002; Aller and Unger, 2006). Recent reports suggest that mammalian Ctr1 is constitutively recycling from an endosomal compartment to the plasma membrane and is stimulated to undergo Cu-specific and rapid clathrin-dependent endocytosis at Cu concentrations near the K_m for transport (Petris et al., 2003; Guo et al., 2004). While Ctr1 is localized to the plasma membrane in many cultured cell lines, Ctr1 also localizes to intracellular vesicular compartments in other cells, perhaps reflecting distinct differences in Cu status or the endocytic machinery (Klomp et al., 2002). In response to high Cu concentrations, Ctr1 endocytosis leads to degradation, potentially providing a rapid and Cu-specific mechanism to regulate Ctr1-mediated high-affinity Cu uptake (Petris et al., 2003; Guo et al., 2004).

Little is known about the physiological role of Ctr1 in dietary Cu acquisition in mammals and in Cu delivery to peripheral tissues. Interestingly, *Ctr1*^{+/-} mice exhibit no obvious growth or developmental abnormalities. However, these mice do exhibit tissue-specific reductions in Cu accumulation and in Cu-dependent enzyme activities in brain and spleen (Lee et al., 2001; Kuo et al., 2001). Moreover, *Ctr1*^{-/-} mice are embryonic lethal, with embryos exhibiting poor growth rates and defects in development of neural ectoderm and mesoderm (Lee et al., 2001; Kuo et al., 2001). *Ctr1*^{-/-} fibroblasts exhibit an $\sim 70\%$ reduction in Cu uptake and accumulation compared to wild-type cells but also express a biochemically distinct Cu uptake activity of a lower affinity ($K_m \sim 10 \mu\text{M}$) that appears to transport Cu(II), rather than Cu(I) (Lee et al., 2002b).

To determine whether Ctr1 might function in intestinal Cu acquisition, we generated a mouse model in which the Ctr1 locus is excised specifically and efficiently in intestinal epithelial cells. These mice exhibit striking early postnatal defects in growth, peripheral Cu accumulation, and the activities of Cu-dependent enzymes; a profound hepatic Fe hyperaccumulation; pronounced cardiac hypertrophy; and other pathologies. Surprisingly, these animals can be rescued with a single Cu administration to the periphery, indicating a critical requirement for Ctr1-mediated intestinal Cu absorption in neonates. Moreover, intestinal epithelial cells from Ctr1 intestinal epithelial knockout mice demonstrated an unexpected and dramatic hyperaccumulation of Cu that is not biologically available, suggesting a critical role for Ctr1 in Cu metabolism both at the plasma membrane and potentially in an intracellular compartment.

Results

Generation of an intestinal epithelial *Ctr1* knockout mouse model

To ascertain if Ctr1 may function in intestinal Cu absorption, immunohistochemistry was carried out on mouse intestinal duodenal cross-sections (Figure 1A). While no specific signal was detected in the absence of antibody (data not shown), affinity-purified anti-Ctr1 antibody showed a clear staining of the apical membrane of intestinal epithelial cells, with an increase in expression from the crypt to the tip of the villus. Other duodenal immunohistochemical analyses of Ctr1 (for example, see Figure 1E), and a recent report (Kuo et al., 2006), indicate both apical membrane staining and Ctr1 localization to intracellular compartments that may be similar to the endosomal compartments previously described (Klomp et al., 2002; Petris et al., 2003).

Ctr1 is at least partially localized to the apical membrane of mouse intestinal epithelial cells and therefore could function in intestinal dietary Cu uptake. Because a systemic Ctr1 knockout is embryonic lethal (Lee et al., 2001; Kuo et al., 2001), we generated a conditional knockout *Ctr1* allele by flanking the entire coding region with loxP recombination sites from the bacteriophage P1 (Sauer, 1998; Nagy, 2000), by homologous recombination in mouse embryonic stem (ES) cells (Nagy et al., 1993). ES cells heterozygous for this allele (Figure 1B) were used for germline transmission manipulations to create a mouse homozygous for the *Ctr1* allele flanked by loxP sites, hereafter referred to as *Ctr1*^{fllox/fllox} (Figure S1 in the Supplemental Data available with this article online). The homozygous *Ctr1* floxed mice appeared in litters at the expected Mendelian frequency and exhibited no obvious growth or developmental defects, and Cu concentrations in brain, heart, liver, kidney, spleen, serum, and isolated intestinal epithelial cells were indistinguishable from wild-type mice (Table S1).

To generate mice specifically depleted for *Ctr1* in intestinal epithelial cells, the *Ctr1*^{fllox/fllox} mice were crossed with a transgenic mouse expressing the nuclear-targeted bacteriophage P1 Cre recombinase driven from a 12.4 kb Villin promoter. Previous studies demonstrated that these mice express Cre enzyme specifically in intestinal enterocytes with increasing levels from the crypt to the tip of the villus along the entire intestinal tract (Madison et al., 2002). *Villin-Cre; Ctr1*^{fllox/fllox} mice were obtained at the expected Mendelian ratio, suggesting the absence of a growth or developmental selection against the inheritance of these alleles. To ascertain the *Ctr1* allele status, tissues from postnatal day 14 (P14) were subjected to PCR genotyping. As shown in Figure 1C, *Ctr1*^{fllox/fllox} mice lacking Cre recombinase exhibited no *Ctr1* excision in any tissue. However, *Ctr1*^{fllox/fllox} mice harboring the *Villin-Cre* transgene had excised *Ctr1* from intestinal epithelial cells (IEC) with high efficiency, with no detectable *Ctr1* excision in brain, heart, liver, kidney, or spleen. These mice are hereafter referred to as *Ctr1*^{int/int} mice, to signify *Ctr1* excision specifically in intestinal epithelial cells. Immunoblotting of membrane extracts from these same tissues revealed undetectable levels of Ctr1 in intestinal epithelial cells of *Ctr1*^{int/int} mice, whereas the levels in control mice were readily detectable and not reduced in other tissues relative to control mice (Figure 1D). Ctr1 levels may be slightly elevated in heart and liver tissue from *Ctr1*^{int/int} mice, perhaps due to a peripheral Cu deficiency (see below) that minimizes Cu-induced

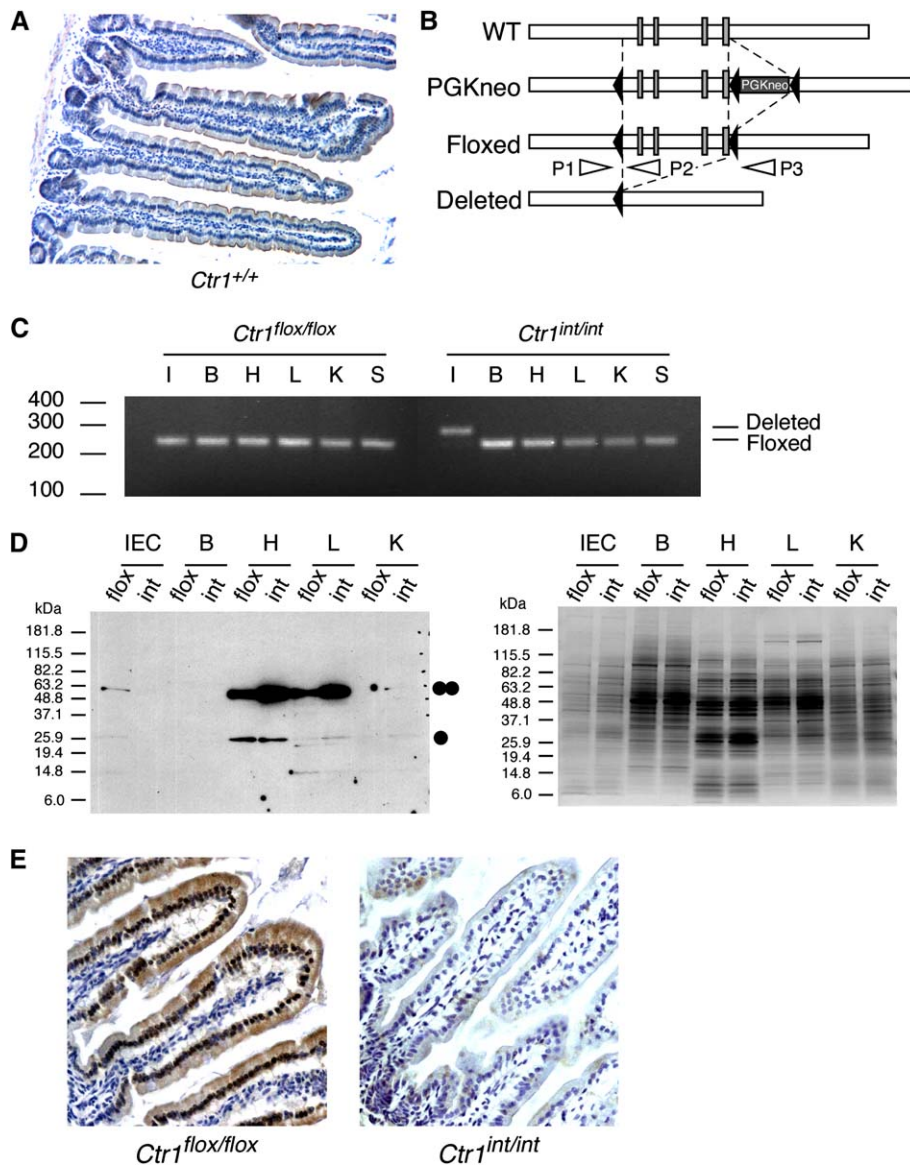


Figure 1. Conditional deletion of *Ctr1* in intestinal epithelia

A) Immunohistochemistry of wild-type (*Ctr1*^{+/+}) mouse duodenum probed with anti-Ctr1 (1:100 dilution). Immunopositive staining (brown) represents the presence of Ctr1 on the apical membrane of the intestinal epithelium.

B) Targeting strategy used for conditional deletion of *Ctr1*. The *Ctr1* structural gene (gray boxes) was flanked by loxP sites (black triangles) followed by the *PGKneo* gene cassette (black box) with an additional loxP site. The *PGKneo* gene was removed by crossbreeding with *EllaCre* mice, and mice having the desired allele of *Ctr1* flanked by loxP (floxed) were obtained. The *Ctr1*-deleted allele (deleted) was obtained by crossbreeding with *Villin-Cre* mice. The locations of the PCR primer (P1, P2, and P3) binding sites used to diagnose Cre-mediated deletion are shown as open arrows.

C) PCR analysis of tissue DNA from *Ctr1*^{flox/flox} and intestinal *Ctr1* knockout (*Ctr1*^{int/int}) mice at postnatal day (P) 14. The PCR product from *Ctr1*^{flox/flox} is 242 bp, whereas the product from *Ctr1*^{int/int} is 281 bp. I, isolated intestinal epithelial cells; B, brain; H, heart; L, liver; K, kidney; S, spleen.

D) Immunoblot analysis of tissue Ctr1 protein. Blots were probed with anti-Ctr1 antibody (1:1000 dilution). flox, *Ctr1*^{flox/flox}, int, *Ctr1*^{int/int}, IEC, isolated intestinal epithelial cells. The Ctr1 homodimer (double closed circle) and monomer form (single closed circle) were detected (left panel). The gel was stained with Coomassie blue (right panel).

E) Immunohistochemistry of *Ctr1*^{flox/flox} and *Ctr1*^{int/int} mouse duodenum with anti-Ctr1 antibody (1:100 dilution).

endocytosis and degradation that has been observed in some cultured cell lines (Klomp et al., 2002; Petris et al., 2003). It is notable that, while the steady-state levels of Ctr1 mRNA and protein are abundant in kidney tissue from mature mice (Lee et al., 2000), Ctr1 protein levels are very low in kidney from these 2-week-old mice. Immunohistochemistry of duodenal villus cross-sections with anti-Ctr1 antibody showed robust staining of Ctr1 on both the apical membrane and on internal compartments that may correspond to previously identified endosomes (Petris et al., 2003; Guo et al., 2004) from wild-type animals, but almost undetectable Ctr1 levels in IEC of *Ctr1*^{int/int} mice (Figure 1E). Taken together, these data demonstrate the generation of a highly efficient and highly specific intestinal epithelial *Ctr1* knockout mouse model.

***Ctr1*^{int/int} mice exhibit growth and peripheral Cu absorption defects**

While *Ctr1*^{int/int} mice were born at the expected frequency and exhibited normal growth rate and mass for the first 6–8 days postpartum, poor growth and lethality occurred beginning

approximately 10 days after birth (Figures 2A and 2B). While the majority of *Ctr1*^{int/int} mice died with severe weight loss (as shown in Figure 2C at day P14, a representative *Ctr1*^{flox/flox} mouse had a mass of approximately 9 grams, while a *Ctr1*^{int/int} mouse weighed less than 4 grams), weight loss was less severe in some mice. Furthermore, while there was nearly 100% lethality for *Ctr1*^{int/int} mice by approximately 3 weeks postpartum, 3 of approximately 110 *Ctr1*^{int/int} mice were asymptomatic. Further analysis of these mice demonstrated very low expression of Cre recombinase and levels of intestinal epithelial Ctr1 protein that were indistinguishable from control mice (data not shown). The *Ctr1*^{int/int} mice also displayed hypopigmentation, skin laxity, ataxia, and brittle, kinky whiskers, reminiscent of the human Cu homeostasis disease known as Menkes kinky hair disease (Lutsenko and Petris, 2002; Llanos and Mercer, 2002) (Figures 2C and 2D).

Since *Ctr1*^{int/int} mice exhibit outward phenotypes consistent with deficits in the activities of Cu-dependent enzymes, the steady-state levels of Cu accumulated in several peripheral tissues were evaluated by ICP-MS and compared to those of

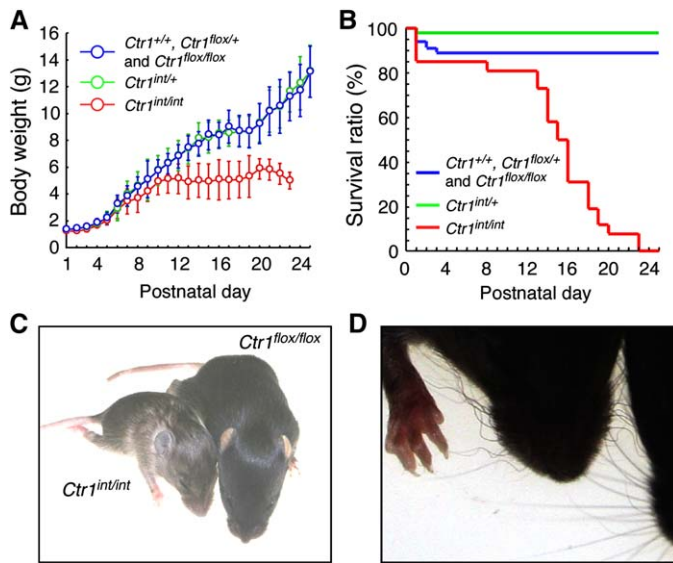


Figure 2. Growth and survival phenotypes of *Ctr1*^{int/int} mice

A and B The growth curve (**A**) (mean \pm SD) and the survival ratio (**B**) of mutant and control mice. Blue, *Ctr1*^{+/+}, *Ctr1*^{flox/+}, and *Ctr1*^{flox/flox} ($n = 57$); green, *Ctr1*^{int/+} ($n = 47$); red, *Ctr1*^{int/int} ($n = 26$). The expected life span of *Ctr1*^{int/int} was 16 ± 4 days (mean \pm SD) ($n = 22$).

C Mouse siblings at P14. Left, *Ctr1*^{int/int}; right, *Ctr1*^{flox/flox}.

D *Ctr1*^{int/int} mice exhibit kinky whiskers.

control mice. As shown in Figure 3A, Cu accumulation in all peripheral tissues evaluated was significantly reduced compared to control littermates, with severe reductions in liver (~5%), heart (~18%), and brain (~20%) as compared to control animals. Spleen and serum Cu levels were under 40% the levels of control mice. Interestingly, Cu levels from *Ctr1*^{int/int} kidney were reproducibly 70% or more that of the kidney from control animals. Furthermore, while tissue Zn levels were not significantly altered as compared to control mice (Figure 3B), liver Fe levels were strongly elevated more than 4-fold over those of control mice, with smaller changes in other tissues (Figure 3C). Consistent with Fe hyperaccumulation, IEC and liver but not kidney from *Ctr1*^{int/int} mice also exhibited dramatically elevated levels of the Fe storage protein ferritin as compared to control littermates (Figure 3D). To ascertain which liver cell types accumulate Fe in *Ctr1*^{int/int} mice, liver sections were stained with Perl's Prussian blue and visualized by light microscopy. While no significant Fe deposits were detected by this method in control liver samples, liver from *Ctr1*^{int/int} mice accumulated Fe predominantly in Kupffer cells (Figure 3E).

The severe growth defects of *Ctr1*^{int/int} mice, coupled with significant reductions in Cu accumulation in peripheral tissues and gross hepatic Fe accumulation, would predict deficits in cellular enzymatic activities or regulatory events that are dependent on Cu. Indeed, mitochondrial cytochrome oxidase activity was severely decreased in total brain, heart, and liver lysates of *Ctr1*^{int/int} mice as compared to control littermates (Figure 4A); these same tissues exhibited the most profound Cu deficits. Moreover, in line with Cu accumulation measurements (Figure 3A), no significant change in cytochrome oxidase activity was observed in kidney. Consistent with the hypopigmentation phenotype of *Ctr1*^{int/int} mice, skin extracts from these mice exhibit reduced levels of tyrosinase activity (Figure 4B).

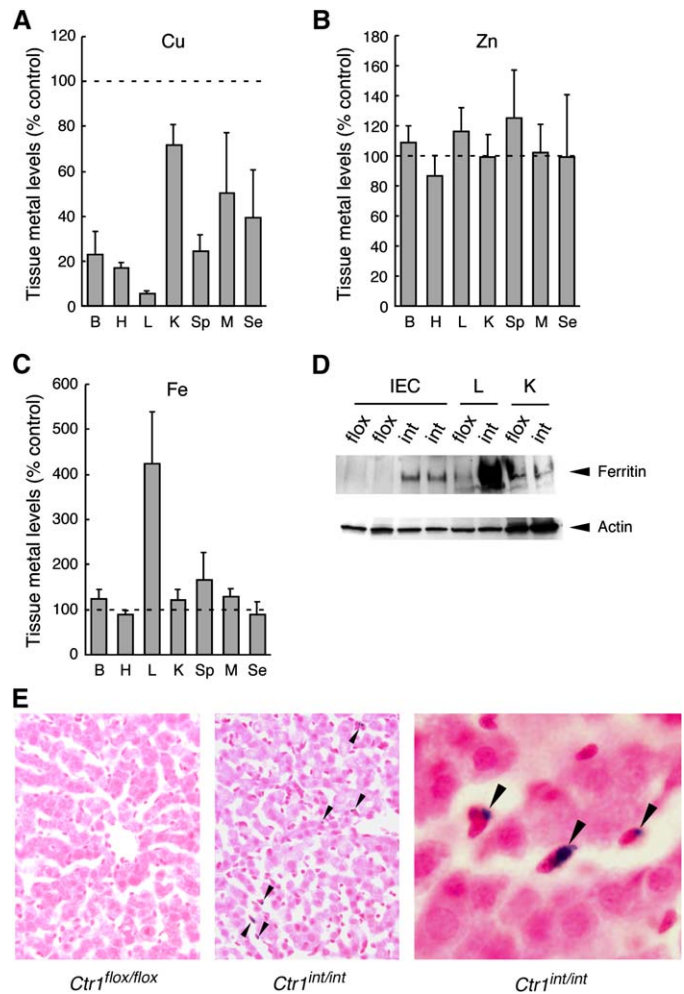


Figure 3. Peripheral Cu hypoaccumulation and hepatic Fe hyperaccumulation in *Ctr1*^{int/int} mice

A–C Relative Cu (**A**), Zn (**B**), and Fe (**C**) concentrations were measured in each tissue of *Ctr1*^{int/int} ($n = 6$) compared to control (*Ctr1*^{flox/+} and *Ctr1*^{flox/flox}) ($n = 6$) mice by ICP-MS. Data are represented as the percent of metal concentration (μg metal/mg tissue wet weight) in mutant mouse tissues compared to those of control (average \pm SD). B, brain; H, heart; L, liver; K, kidney; Sp, spleen; M, skeletal muscle; Se, serum. Dashed lines represent 100% of each metal in control mouse tissues. **D** Immunoblot of ferritin from IEC, liver, and kidney protein extracts derived from *Ctr1*^{flox/flox} and *Ctr1*^{int/int} mice. The positions of ferritin and the actin loading control are indicated with arrowheads.

E Perl's staining of liver sections from *Ctr1*^{flox/flox} and *Ctr1*^{int/int} mice. The left (*Ctr1*^{flox/flox}) and middle (*Ctr1*^{int/int}) panels show lower magnification of liver sections. Iron deposits were observed in *Ctr1*^{int/int} liver as blue spots (arrowheads). The right panel shows a higher magnification of a *Ctr1*^{int/int} liver section. Iron deposits were observed in Kupffer cells (arrowheads). Cytosol and nuclei are counterstained with pararosaniline.

A well-characterized Cu-dependent enzyme, Cu,Zn superoxide dismutase (SOD1), is Cu metallated in yeast and mammals via the action of the CCS Cu chaperone (Rae et al., 1999; Wong et al., 2000; Schmidt et al., 2000). While previous studies have demonstrated that Cu-deficient animal models exhibit clear deficiencies in SOD1 activity (Prohaska et al., 2003), recent studies have demonstrated that steady-state CCS levels are inversely proportional to intracellular Cu availability due to 26S proteasome-dependent degradation in a highly specific manner (Bertinato and L'Abbé, 2003; West and Prohaska, 2004; Caruano-Yzermans et al., 2006). We evaluated steady-state CCS

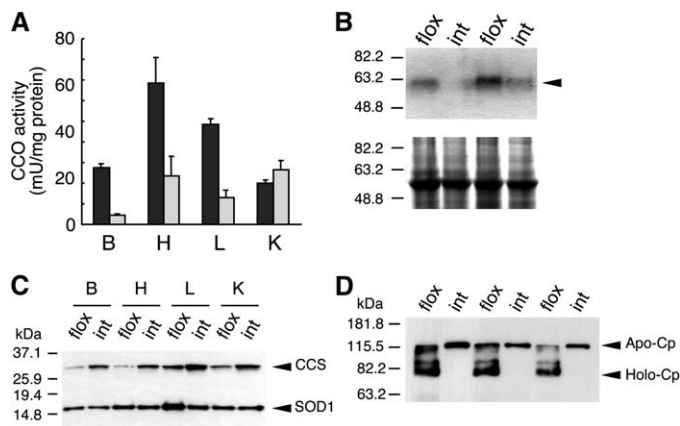


Figure 4. *Ctr1*^{int/int} mice exhibit biochemical signatures of Cu deficiency

A) Cytochrome c oxidase (CCO) activity. Tissue extracts from three control (*Ctr1*^{flox/+} and *Ctr1*^{flox/flox}) and three *Ctr1*^{int/int} mice were used to measure CCO activity. Data are represented as mU/mg protein (mean + SD) (n = 3). B, brain; H, heart; L, liver; K, kidney. Dark bars represent CCO activity from control mice, and light bars represent CCO activity from *Ctr1*^{int/int} mice.

B) Skin tyrosinase activities. The arrowhead indicates tyrosinase activity. The gel was stained with CBB to control for protein loading (lower panel). flox, *Ctr1*^{flox/flox}; int, *Ctr1*^{int/int}.

C) Immunoblot for copper chaperone for superoxide dismutase (CCS) steady-state levels. The membrane was probed with anti-CCS antibody at 1:200 dilution. Cu,Zn-superoxide dismutase (SOD1) is shown as a loading control. B, brain; H, heart; L, liver; K, kidney. flox, *Ctr1*^{flox/flox}; int, *Ctr1*^{int/int}.

D) Ceruloplasmin (Cp) Cu metallation assays. One microliter serum from three *Ctr1*^{flox/flox} and three *Ctr1*^{int/int} mice was subjected to nonreducing SDS-PAGE and immunoblotting with anti-human Cp antibody. flox, *Ctr1*^{flox/flox}; int, *Ctr1*^{int/int}. Arrows indicate the positions of the apo-Cp and holo-Cp polypeptides.

levels as an indicator of endogenous bioavailable Cu levels and compared CCS levels in several tissues in control and *Ctr1*^{int/int} mice. As shown by immunoblotting with anti-CCS antiserum in Figure 4C, the CCS steady-state levels increased significantly in each tissue from the *Ctr1*^{int/int} mice as compared to control littermates. The increase in CCS steady-state levels was also observed in kidney, indicating that even modest perturbation of steady-state Cu accumulation alters CCS proteolysis. This suggests that changes in CCS levels may be a more sensitive reflection of bioavailable Cu levels than the analysis of Cu-dependent enzymes. Due to the structural similarity between SOD1 and the central domain of mammalian CCS (Lamb et al., 2000; Huffman and O'Halloran, 2001), the antibody used for immunoblotting shown in Figure 4C also crossreacts with SOD1. While the liver sample shows elevated SOD1 levels in control liver samples relative to the *Ctr1*^{int/int} mouse, this is not reproducible in other experiments, and this particular lane was overloaded.

The multicopper ferroxidase ceruloplasmin is a serum glycoprotein that is synthesized and matured in the liver and secreted in the serum, where it functions in Fe(III) loading onto transferrin for distribution to peripheral tissues (Andrews, 2000; Hellman and Gitlin, 2002; Kaplan, 2002). Furthermore, a recent report suggests that ceruloplasmin also functions in Fe efflux from intestinal enterocytes (Cherukuri et al., 2005). While Cu deficiency in cell culture and in vivo does not alter ceruloplasmin protein synthesis, these conditions are known to severely compromise the incorporation of seven Cu atoms into the protein as it traverses the secretory pathway (Sato and Gitlin, 1991; Hellman et al., 2002). Because of the severe hepatic Cu depletion in *Ctr1*^{int/int} mice, we evaluated ceruloplasmin metallation state

using nonreducing SDS-PAGE and immunoblotting. As shown in Figure 4D, while serum from control littermates harbors predominantly holo-ceruloplasmin, with low levels of apo-protein, serum from *Ctr1*^{int/int} mice resolves almost exclusively apo-ceruloplasmin, with holo-ceruloplasmin detectable only upon overexposure of the immunoblot (data not shown). Taken together, tissue steady-state Cu accumulation measurements, Cu-dependent enzyme activity deficits, increased CCS levels, and decreased ceruloplasmin Cu loading in *Ctr1*^{int/int} mice as compared to the control littermates demonstrate that *Ctr1* plays a highly significant role in mammalian intestinal Cu absorption.

Cardiac hypertrophy associated with *Ctr1*^{int/int} mice

Animal models of dietary Cu deficiency demonstrate clear defects in angiogenesis, impaired aortic elasticity, and cardiac hypertrophy (Linder, 1991; Jauby et al., 1998; Prohaska and Brokate, 2002; Elsherif et al., 2003). This latter condition is thought to be accompanied by mitochondrial volume increases that ultimately lead to large vacuolar mitochondrial structures in which cristae have lost the typical parallel array (Elsherif et al., 2004). As shown in Figure 2C, P14 *Ctr1*^{int/int} mice are profoundly smaller than control littermates. Accordingly, the mass ratio (wet weight/total body mass) of several tissues including spleen was significantly smaller for the mutant mouse (Figure 5A), whereas there was no significant difference in the mass ratio of the kidney comparing six control and six mutant mice. Interestingly, the heart mass ratio was significantly increased in *Ctr1*^{int/int} mice compared to control littermates (n = 10), where there was an average ~20% increase in heart mass relative to total body mass. Hematoxylin and eosin staining of heart sections revealed abundant large vacuoles in cardiac tissue from the *Ctr1*^{int/int} mice, but not in cardiac tissue from control littermates (Figure 5B). Electron microscopic evaluation of thin sections of fixed cardiac tissue from these mice showed a regular array of mitochondria-packed cells in control tissue, whereas *Ctr1*^{int/int} cardiac tissue exhibited swollen, pale mitochondria and features consistent with the vacuoles being derived from swollen mitochondria harboring disordered cristae (Figures 5C and 5D). Taken together, these studies demonstrate that the peripheral Cu deficiency due to loss of intestinal epithelial cell *Ctr1* leads to cardiac hypertrophy within 2 weeks after birth.

Ctr1^{int/int} intestinal epithelial cells hyperaccumulate Cu

Our data support the notion that, normally, *Ctr1* transports dietary Cu across the apical membrane, whereupon it is utilized intracellularly and pumped across the basolateral membrane, to the portal circulation, via the Cu-transporting ATPase ATP7A. We analyzed the Cu content of purified intestinal epithelial cells from *Ctr1*^{int/int} mice and control littermates. Unexpectedly, purified IEC from *Ctr1*^{int/int} mice accumulated over eight times the levels of Cu as compared to IEC from control littermates (Figure 6A). Fe or Zn levels were not significantly elevated in these cells compared to control IEC. To explore whether these highly elevated Cu levels are available to drive Cu-dependent enzymatic and regulatory events, several markers of intracellular bioavailable Cu were analyzed. As shown in Figure 6B, steady-state levels of CCS are strongly elevated in *Ctr1*^{int/int} IEC compared to control cells, with no change in steady-state SOD1 protein. Recent studies have also demonstrated that hephaestin, a Cu-dependent ferroxidase localized to the basolateral membrane of IEC and expressed in kidney that facilitates Fe export,

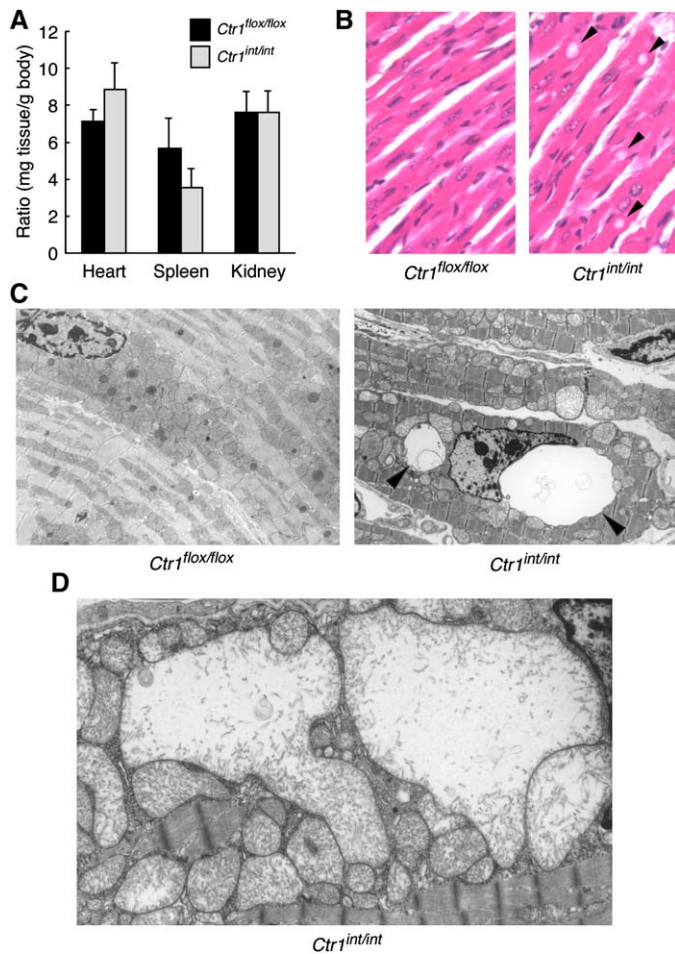


Figure 5. *Ctrl^{int/int}* mice exhibit cardiac hypertrophy 2 weeks postpartum

A) The organ/body mass ratio of mutant (*Ctrl^{int/int}*) mice is compared to that of control (*Ctrl^{flox/flox}*) mice (mean + SD) (n = 10) (p < 0.01). **B)** *Ctrl^{int/int}* mouse cardiac tissue histology. Mouse heart sections were stained with hematoxylin and eosin. Left panel: *Ctrl^{flox/flox}*, right panel: *Ctrl^{int/int}*. Vacuole structures are indicated with arrowheads. **C)** Electron microscopy of cardiac tissue. Left panel (*Ctrl^{flox/flox}*) and right panel (*Ctrl^{int/int}*) are 3000x magnifications of heart thin sections. The contrast of those two pictures is different to show the structural details of mitochondria. **D)** Cardiac thin section electron micrographs from *Ctrl^{int/int}* mice showing vacuoles containing cristae structures.

is regulated by Cu levels in a direction opposite to that of CCS (Nittis and Gitlin, 2004). Steady-state hephaestin protein levels are elevated by Cu and reduced in Cu-deficient cells. As shown in Figure 6C, IEC from *Ctrl^{int/int}* mice have reduced hephaestin levels relative to that from control mice. Furthermore, levels of

hephaestin were unchanged in kidney, a tissue in which steady-state Cu levels did not change dramatically. The opposing regulation of CCS and hephaestin observed in *Ctrl^{int/int}* mice is consistent with a reduction in Cu that is available to signal the proteolysis of CCS and hephaestin (Bertinato and L'Abbé, 2003; Nittis and Gitlin, 2004; West and Prohaska, 2004; Caruano-Yzermans et al., 2006). To further test this notion, the levels of cytochrome oxidase activity were measured in IEC isolated from *Ctrl^{int/int}* mice and from control littermates. As shown in Figure 6D, cytochrome oxidase activity was reduced approximately 3-fold in *Ctrl^{int/int}* IEC cells compared to control cells. Taken together, these results demonstrate that, while intestinal epithelial cell *Ctrl1* is essential for dietary acquisition of Cu for delivery to peripheral tissues, it is also required to prevent the hyperaccumulation of Cu in IEC in an as yet unidentified biologically unavailable pool.

Bypassing intestinal Cu absorption rescues *Ctrl^{int/int}* mice

To further test whether the growth, biochemical, and pathological phenotypes observed in *Ctrl^{int/int}* mice are due to a critical role for *Ctrl1* in dietary Cu absorption, we attempted to bypass intestinal Cu absorption. *Ctrl^{int/int}* or control mice at day P5 or P6 were given an intraperitoneal (IP) injection of 10 μg/g total body mass of CuSO₄ in 10 μl of physiological saline, or saline alone, and monitored for growth rate and survival. Control mice were unaffected by the injection of saline or copper (Figure 7A). Three *Ctrl^{int/int}* mice injected with saline alone showed early postnatal lethality, with or without progressive weight loss, by postnatal day 20 (Figure 7B, open circles), similar to that observed for the *Ctrl^{int/int}* mice shown in Figure 2B. In contrast, all three *Ctrl^{int/int}* mice receiving a single IP copper injection demonstrated neither weight loss nor early postnatal death. One or two mice from an independent copper rescue experiment were sacrificed for analysis of heart/body mass ratio, cardiac tissue histology, and tissue copper levels. This preliminary analysis suggested that the cardiac hypertrophy (heart/body mass ratio) and vacuoles observed in *Ctrl^{int/int}* mice treated with saline were partially reversed with copper treatment (data not shown). Furthermore, *Ctrl^{int/int}* mice injected with copper showed a trend toward restoration of copper levels in peripheral tissues, though these analyses are not statistically significant due to availability of only one or two animals. Two of the copper-injected *Ctrl^{int/int}* mice described in Figure 7B are currently 5 months old and appear outwardly asymptomatic. Interestingly, as described for a few atypical mice for Figure 2B, one *Ctrl^{int/int}* mouse injected with saline demonstrated neither progressive weight loss nor early postnatal lethality (Figure 7B). Upon evaluation this mouse expressed low levels of Cre recombinase and normal

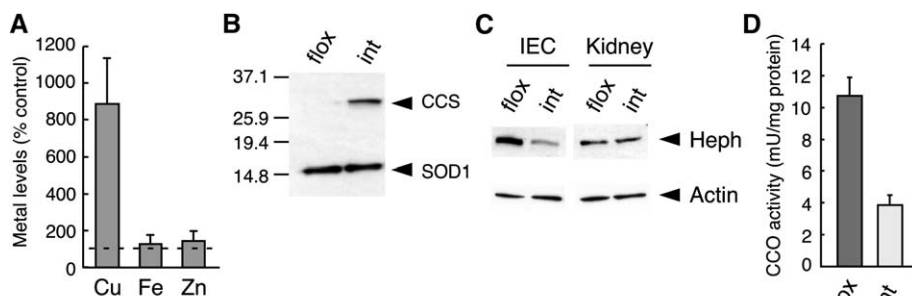


Figure 6. Hyperaccumulation of Cu by *Ctrl^{int/int}* IEC **A)** Relative Cu, Fe, and Zn levels associated with *Ctrl^{int/int}* IEC compared to those of control (*Ctrl^{flox/flox}*) cells. Data are represented as percent of control cells (mean + SD) (n = 6). Wild-type levels are indicated with a dashed line. **B)** CCS levels (with SOD1 as loading control). **C)** Hephaestin levels in IEC and from kidney were detected by immunoblotting with anti-hephaestin antibody at 1:1000 dilution. Heph and Actin are indicated with arrowheads. **D)** Cytochrome c oxidase activity was assayed in IEC as described for Figure 4 (mean + SD) (n = 3).

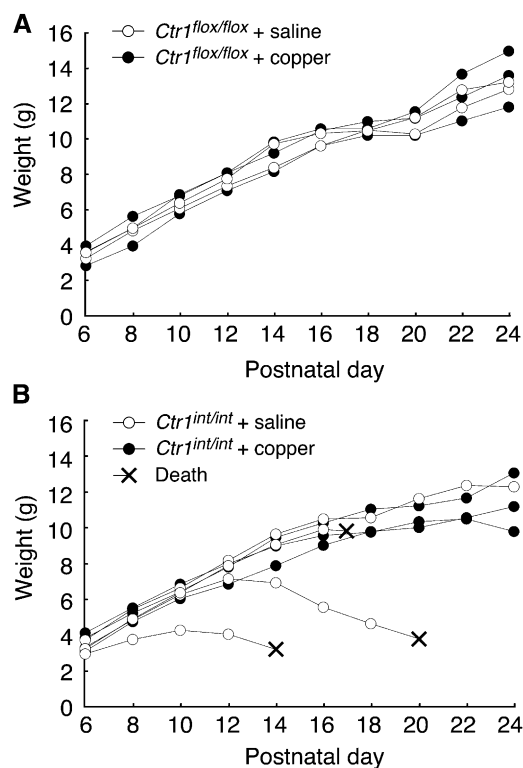


Figure 7. Rescue of $Ctr1^{int/int}$ mice with a single intraperitoneal Cu administration. Mice were given a single IP injection with $10 \mu\text{g CuSO}_4/\text{g}$ body weight in $10 \mu\text{l}$ of physiological saline or saline alone at P5 or P6, and mass was determined each day. Weight (g) of control (Figure 7A) and $Ctr1^{int/int}$ (Figure 7B) mice administered saline or copper was plotted against time (postnatal day). Each growth curve corresponds to an individual mouse. Open circle, saline; closed circle, copper; X, death.

levels of Ctr1 protein in IEC. Taken together, these copper remediation experiments demonstrate the ability to rescue the growth and early postnatal lethality associated with loss of intestinal epithelial Ctr1. Furthermore, the experimental results shown in this report firmly establish the importance of the Cu import activity of Ctr1 in intestinal epithelial cells, rather than some as yet unidentified Ctr1-dependent activity.

Discussion

Cu metabolism is essential to drive biochemical reactions critical for growth, development, cognition, and a host of other key life processes. While all Cu acquisition is thought to occur via dietary absorption in the small intestine, pivotal molecules that mediate Cu uptake in the intestine had not been identified. In this work we demonstrate that Ctr1 is expressed *in vivo* in intestinal epithelial cells on the apical membrane and in intracellular vesicular compartments, consistent with previous Ctr1 localization studies in a range of cultured cell lines (Lee et al., 2002a; Klomp et al., 2002). Ctr1 has previously been demonstrated to function in metal-specific high-affinity Cu uptake while residing on the plasma membrane of distinct mammalian and insect cell lines (Lee et al., 2002a; Puig et al., 2002; Eisses et al., 2005). Transfection studies expressing epitope-tagged versions of Ctr1 have shown that, while Ctr1 undergoes constitutive recycling to and from the plasma membrane, it is rapidly endocytosed in response to elevated Cu concentration, but not other metals

(Petris et al., 2003). Ctr1 endocytosis is dependent on functionally important methionine residues that are conserved from yeast to humans and is clathrin dependent, and Ctr1 colocalizes in intracellular vesicles containing transferrin (Petris et al., 2003; Guo et al., 2004). Our data localize endogenous mouse Ctr1 to both the apical membrane and intracellular compartments of intestinal epithelial cells and suggest that Ctr1 may cycle to and from the plasma membrane in these cells. Further studies will be necessary to ascertain whether Ctr1 is subject to Cu-stimulated endocytosis in intestinal epithelial cells and if this regulatory mechanism is responsible for the previous observation that copper loading decreased the efficiency of dietary copper uptake (Turnlund, 1998).

An unanticipated observation from our studies was that IEC from $Ctr1^{int/int}$ mice accumulate Cu, but not other metals, at levels eight to ten times that of IEC from control animals. Given the dramatic rise in CCS steady-state levels, the strong reduction in hephaestin protein levels and in mitochondrial cytochrome oxidase activity, these observations support the notion that the elevated Cu associated with these cells is not bioavailable. Attempts to strip Cu from the surface of purified intact IEC with strong Cu chelators, or to shave bound extracellular Cu with proteases, were unsuccessful (data not shown), suggesting the possibility that these cells hyperaccumulate intracellular Cu in a form or compartment where it cannot be utilized. Since Ctr1, like DMT1, localizes to the plasma and apical membrane, as well as intracellular vesicles (Andrews, 2000; Gunshin et al., 2005a), these observations suggest the possibility that Ctr1 functions to transport Cu both across the plasma membrane and from the lumen of as yet unidentified intracellular compartments. Alternatively, Ctr1 could function to transport copper in a two step process that could entail binding of Cu(I) at the cell surface, followed by mobilization of Cu from endosomal compartments in which Cu may accumulate in $Ctr1^{int/int}$ IEC. In either case these data clearly demonstrate a crucial role for intestinal Ctr1 in dietary copper absorption.

Given the established preference of yeast and mammalian Ctr1 for Cu(I) transport, these studies suggest that Cu(I) is a principal ionic species acquired through the diet. Furthermore, these observations would predict the expression of one or more metalloreductases in intestinal epithelial cells that would function in concert with Ctr1. The recent identification of DcytB as an intestinal brush border Fe (III) reductase is one candidate that is strongly expressed in response to Fe deficiency (McKie et al., 2001). While mouse Dcytb systemic knockout studies have not revealed an Fe acquisition defect, it is possible that DcytB functions in dietary Cu acquisition (Gunshin et al., 2005b). It is also interesting that a family of mammalian proteins bearing structural similarity to the yeast FRE family of Fe(III)/Cu(II) reductases has recently been identified that could functionally interact with Ctr1 (Ohgami et al., 2005, 2006).

$Ctr1^{int/int}$ mice exhibit severe early postnatal growth and viability defects, perhaps reflecting the depletion of maternal Cu stores. Here, we demonstrated that the early postnatal viability defect associated with $Ctr1^{int/int}$ mice could be partially suppressed via IP Cu administration. These results are consistent with a critical role for Ctr1 in intestinal Cu absorption, rather than another, as yet unidentified function for Ctr1. While our data with only a few mice suggest that this single copper administration may also partially reverse deficits in peripheral copper accumulation and cardiac hypertrophy, it is possible that higher

Cu doses or repeated Cu administration could more completely reverse defects associated with the *Ctr1^{int/int}* mouse. More extensive studies will be needed to comprehensively test this. It is interesting that mice lacking IEC *Ctr1* show such a significant accumulation of hepatic Fe only 2 weeks after birth. Given the requirement for Cu in ceruloplasmin-mediated Fe(III) loading onto the transferrin receptor, and for hephaestin-facilitated Fe efflux thought to occur in rat liver Kupffer cells (Zhang et al., 2004), this observation further underscores the early postnatal requirement for Cu in normal liver Fe metabolism.

Experimental procedures

Generation of *Ctr1^{int/int}* mice

Details on the generation of mice containing the *Ctr1^{flox}* allele are described in the Supplemental Data. *Ctr1^{flox/flox}* mice were crossbred with *Villin-Cre* mice (Jackson Laboratory) to make *Villin-Cre; Ctr1^{flox/+}* mice. The male *Villin-Cre; Ctr1^{flox/+}* mice were crossbred with female *Ctr1^{flox/flox}* mice, and *Ctr1^{int/int}* mice were obtained. Genotyping of *Ctr1* was carried out by standard approaches using PCR with the forward primer P1 (5'-AATGTCCTGGTGCCTGAAA-3') and the reverse primer P2 (5'-GCAGTAGATAAAAGCCAAGGC-3'). To detect tissue excision of *Ctr1* by Cre recombinase, PCR with three primers, P1, P2, and P3 (5'-AAAAACCACTATTTCAGAGACTG-3') was performed.

Tissue and cell preparation

Tissues were dissected after perfusion with phosphate-buffered saline (pH 7.4; PBS), frozen in liquid nitrogen, and stored at -80°C until use. Duodenal, liver, and cardiac tissue was fixed immediately after dissection. Intestinal epithelial cells were isolated from mesenchyme by two independent methods. The small intestine was opened along the long axis, washed in ice-cold PBS, and soaked in cell recovery solution (BD Biosciences, Franklin Lakes, NJ) containing protease inhibitors at 4°C overnight with gentle agitation (Pereault and Beaulieu, 1998). Alternatively, washed small intestine was soaked in PBS containing 1.5 mM EDTA and protease inhibitors at 4°C for 10 min with gentle agitation (Chen et al., 2003). After incubation the mesenchyme layer was removed, and intestinal epithelial cells were washed three times with ice-cold PBS with protease inhibitors and recovered by centrifugation at $200 \times g$ for 7 min. Detailed methods for protein extract preparation from tissues or cells are provided in the Supplemental Experimental Procedures.

Immunological techniques

A synthetic peptide of the sequence H₂N-VSIRYNSMPVPGPNGTILC-CO₂H, which corresponds to the cytosolic loop between transmembrane domains 1 and 2 of mouse and human *Ctr1*, was used as antigen for generation and affinity purification of rabbit polyclonal antiserum by Bethyl Laboratories, Inc. (Montgomery, TX).

Tissue metal measurements

Copper, iron, and zinc concentrations were measured from nitric acid-digested tissues by inductively coupled plasma mass spectrometry (ICP-MS) as described (Lee et al., 2001). The values were normalized by tissue wet weight or protein concentration.

Tissue histology

After perfusion, dissection and mass determination tissues were fixed in neutralized 4% paraformaldehyde in PBS at 4°C overnight with gentle agitation. After fixation, hearts were transferred into 70% ethanol, dehydrated, and embedded in paraffin. Four micrometer thick sections were made and stained with hematoxylin and eosin. For electron microscopy, heart tissue was minced into approximately 1 mm square cubes in 3% glutaraldehyde immediately after dissection and incubated in the same solution at 4°C overnight. Sectioning, staining, microscopy, and image capture were carried out via the Department of Pathology, Duke University Medical Center (Durham, NC). Perl's Prussian blue staining was carried out on perfused livers that were fixed in neutralized 4% paraformaldehyde in PBS at 4°C overnight with gentle agitation. After fixation livers were transferred to 70% ethanol, dehydrated, and embedded in paraffin. Six micrometer sections were stained with the Iron Stain Kit (Sigma, St. Louis, MO).

Enzyme assays

Tissues were homogenized in five to ten times volume of 50 mM phosphate buffer (pH 6.8) containing 0.5% Tween 80 in 1.5 ml tubes and incubated on ice for 10 min. The homogenates were centrifuged at $16,000 \times g$ for 20 min at 4°C . Protein concentrations were measured by the BioRad Protein DC Assay kit (BioRad) with bovine serum albumin as a standard, and cytochrome oxidase activity was measured using a Cytochrome c Oxidase Assay Kit (Sigma). For tyrosinase assays, mouse skin biopsies were minced; homogenized in 62.5 mM Tris-HCl (pH 6.8), 2% SDS, 1 mM ascorbate, 1 mM BCS, and protease inhibitors on ice; and incubated on ice for 1 hr. The homogenate was centrifuged at $5000 \times g$ for 5 min at 4°C , and the supernatant was further centrifuged at $16,000 \times g$ for 20 min. The supernatant was subjected to protein assays, 60 μg of skin extract was subjected to nonreducing SDS-PAGE, and tyrosinase activity was measured by in-gel colorimetric assays as described (Lee et al., 2002b).

Copper supplementation

Ctr1^{int/int} and *Ctr1^{flox/flox}* (P5 or P6) mice were weighed and administered copper or vehicle. Ten micrograms of copper sulfate per gram of body weight in 10 μl of 0.9% sodium chloride was injected into the IP cavity using a 10 μl syringe (Hamilton 80366) (Hamilton, Reno, NV). For the vehicle control, 10 μl of 0.9% sodium chloride was administered in the same manner. Body weight was monitored each day. At P14, mice from each group were sacrificed, and cardiac tissue histology, metal levels, and ceruloplasmin Cu loading were analyzed as described above.

Supplemental data

Supplemental Data include Supplemental Experimental Procedures, one supplemental table, and one supplemental figure and can be found with this article online at <http://www.cellmetabolism.org/cgi/content/full/4/3/235/DC1/>.

Acknowledgments

We thank Jonathan Gitlin for anti-CCS and hephaestin antiserum and Mick Petris for the tyrosinase activity assay protocol. We are grateful to members of the Thiele laboratory for critical reading of this manuscript, Kelly McNaughton for expert technical assistance, Charles Steenbergen for advice on cardiac histology, and Deb Gumucio for advice with *villin-Cre* mice. This work was supported by grants from the National Institutes of Health (DK074192) and the International Copper Association, Ltd. to D.J.T. The production of ^{64}Cu at Washington University School of Medicine is supported by a grant from the NIH-NCI R24 CA86307.

Received: April 27, 2006

Revised: July 12, 2006

Accepted: August 18, 2006

Published: September 5, 2006

References

- Aller, S.G., and Unger, V.M. (2006). Projection structure of the human copper transporter CTR1 at 6-Å resolution reveals a compact trimer with a novel channel-like architecture. *Proc. Natl. Acad. Sci. USA* 103, 3627–3632.
- Andrews, N.C. (2000). Iron homeostasis: Insights from genetics and animal models. *Nat. Rev. Genet.* 1, 208–217.
- Arredondo, M., Muñoz, P., Mura, C.V., and Núñez, M.T. (2003). DMT1, a physiologically relevant apical Cu¹⁺ transporter of intestinal cells. *Am. J. Physiol.* 284, C1525–C1530.
- Bertinato, J., and L'Abbé, M.R. (2003). Copper modulates the degradation of copper chaperone for Cu,Zn superoxide dismutase by the 26 S proteasome. *J. Biol. Chem.* 278, 35071–35078.
- Caruano-Yzermans, A.L., Bartnikas, T.B., and Gitlin, J.D. (2006). Mechanisms of the copper-dependent turnover of the copper chaperone for superoxide dismutase. *J. Biol. Chem.* 281, 13581–13587.

- Chen, H., Su, T., Attieh, Z.K., Fox, T.C., McKie, A.T., Anderson, G.J., and Vulpe, C.D. (2003). Systemic regulation of Hephaestin and Ireg1 revealed in studies of genetic and nutritional iron deficiency. *Blood* 102, 1893–1899.
- Cherukuri, S., Potla, R., Sarkar, J., Nurko, S., Harris, Z.L., and Fox, P.L. (2005). Unexpected role of ceruloplasmin in intestinal iron absorption. *Cell Metab.* 2, 309–319.
- Eisses, J.F., Chi, Y., and Kaplan, J.H. (2005). Stable plasma membrane levels of hCTR1 mediate cellular copper uptake. *J. Biol. Chem.* 280, 9635–9639.
- Elsherif, L., Ortines, R.V., Saari, J.T., and Kang, Y.J. (2003). Congestive heart failure in copper-deficient mice. *Exp. Biol. Med.* 228, 811–817.
- Elsherif, L., Wang, L., Saari, J.T., and Kang, Y.J. (2004). Regression of dietary copper restriction-induced cardiomyopathy by copper repletion in mice. *J. Nutr.* 134, 855–860.
- Ferruzza, S., Sambuy, Y., Ciriolo, M.R., Martino, A.D., Santaroni, P., Rotilio, G., and Scarino, M.L. (2000). Copper uptake and intracellular distribution in the human intestinal Caco-2 cell line. *Biometals* 13, 179–185.
- Fox, P.L. (2003). The copper-iron chronicles: The story of an intimate relationship. *Biometals* 16, 9–40.
- Gunshin, H., Mackenzie, B., Berger, U.V., Gunshin, Y., Romero, M.F., Boron, W.F., Nussberger, S., Gollan, J.L., and Hediger, M.A. (1997). Cloning and characterization of a mammalian proton-coupled metal-ion transporter. *Nature* 388, 482–488.
- Gunshin, H., Fujiwara, Y., Custosio, A.O., DiRenzo, C., Robine, S., and Andrews, N.C. (2005a). Slc11a2 is required for intestinal iron absorption and erythropoiesis but dispensable in placenta and liver. *J. Clin. Invest.* 115, 1258–1266.
- Gunshin, H., Starr, C.N., DiRenzo, C., Fleming, M.D., Jin, J., Greer, E.L., Sellers, V.M., Galica, S.M., and Andrews, N.C. (2005b). Cybrd1 (duodenal cytochrome b) is not necessary for dietary iron absorption in mice. *Blood* 106, 2879–2883.
- Guo, Y., Smith, K., Lee, J., Thiele, D.J., and Petris, M.J. (2004). Identification of Methionine-rich clusters that regulate copper-stimulated endocytosis of the human Ctr1 copper transporter. *J. Biol. Chem.* 279, 17428–17433.
- Harris, Z.L., Takahashi, Y., Miyajima, H., Serizawa, M., MacGillivray, R.T.A., and Gitlin, J.D. (1995). Aceruloplasminemia: Molecular characterization of this disorder of iron metabolism. *Proc. Natl. Acad. Sci. USA* 92, 2539–2543.
- Hellman, N.E., and Gitlin, J.D. (2002). Ceruloplasmin metabolism and function. *Annu. Rev. Nutr.* 22, 439–458.
- Hellman, N.E., Kono, S., Mancini, G.M., Hoogbeem, A.J., de Jong, G.J., and Gitlin, J.D. (2002). Mechanisms of copper incorporation into human ceruloplasmin. *J. Biol. Chem.* 277, 46632–46638.
- Huffman, D.L., and O'Halloran, T.V. (2001). Function, structure, and mechanism of intracellular copper trafficking proteins. *Annu. Rev. Biochem.* 70, 677–701.
- Kaplan, J. (2002). Mechanisms of cellular iron acquisition: Another iron in the fire. *Cell* 111, 603–606.
- Klomp, A.E.M., Tops, B.B.J., Van Den Berg, I.E.T., Berger, R., and Klomp, L.W.J. (2002). Biochemical characterization and subcellular localization of human copper transporter 1 (hCtr1). *Biochem. J.* 364, 497–505.
- Kuo, Y.M., Zhou, B., Cosco, D., and Gitschier, J. (2001). The copper transporter Ctr1 provides an essential function in mammalian embryonic development. *Proc. Natl. Acad. Sci. USA* 98, 6836–6841.
- Kuo, Y.M., Gybina, A.A., Pyatskowitz, J.W., Gitschier, J., and Prohaska, J.R. (2006). Copper transporter protein (Ctr1) levels in mice are tissue specific and development on copper status. *J. Nutr.* 136, 21–26.
- Lamb, A.L., Wernimont, A.K., Pufahl, R.A., O'Halloran, T.V., and Rosenzweig, A.C. (2000). Crystal structure of the second domain of the human copper chaperone for superoxide dismutase. *Biochemistry* 39, 1589–1595.
- Lee, J., Prohaska, J.R., Dagenais, S.L., Glover, T.W., and Thiele, D.J. (2000). Isolation of a murine copper transporter gene, tissue specific expression and functional complementation of a yeast copper transport mutant. *Gene* 254, 87–96.
- Lee, J., Prohaska, J.R., and Thiele, D.J. (2001). Essential role for mammalian copper transporter Ctr1 in copper homeostasis and embryonic development. *Proc. Natl. Acad. Sci. USA* 98, 6842–6847.
- Lee, J., Peña, M.M.O., Nose, Y., and Thiele, D.J. (2002a). Biochemical characterization of the human copper transporter Ctr1. *J. Biol. Chem.* 277, 4380–4387.
- Lee, J., Petris, M.J., and Thiele, D.J. (2002b). Characterization of mouse embryonic cells deficient in the Ctr1 high affinity copper transporter. *J. Biol. Chem.* 277, 40253–40259.
- Linder, M.C. (1991). *Biochemistry of Copper* (New York: Plenum Press).
- Llanos, R.M., and Mercer, J.F.B. (2002). The molecular basis of copper homeostasis and copper-related disorders. *DNA Cell Biol.* 21, 259–270.
- Luk, E., Jensen, L.T., and Culotta, V.C. (2003). The many highways for intracellular trafficking of metals. *J. Biol. Inorg. Chem.* 8, 803–809.
- Lutsenko, S., and Petris, M.J. (2002). Function and regulation of the mammalian copper-transporting ATPases: Insights from biochemical and cell biological approaches. *J. Membr. Biol.* 191, 1–12.
- Madison, B.B., Dunbar, L., Qiao, X.T., Braunstein, K., Braunstein, E., and Gumucio, D.L. (2002). cis elements of the villin gene control expression in restricted domains of the vertical (crypt) and horizontal (duodenum, cecum) axes of the intestine. *J. Biol. Chem.* 277, 33275–33283.
- McKie, A.T., Barrow, D., Latunde-Dada, G.O., Rolfs, A., Sager, G., Mudaly, E., Mudaly, M., Richardson, C., Barlow, D., Bomford, A., et al. (2001). An iron-regulated ferric reductase associated with the absorption of dietary iron. *Science* 291, 1755–1759.
- Nagy, A. (2000). Cre recombinase: The universal reagent for genome tailoring. *Genesis* 26, 99–109.
- Nagy, A., Rossant, J., Nagy, R., Abranmow-Newerly, W., and Roder, J.C. (1993). Derivation of completely cell culture-derived mice from early-passage embryonic stem cells. *Proc. Natl. Acad. Sci. USA* 90, 8424–8428.
- Nittis, T., and Gitlin, J.D. (2004). Role of copper in the proteasome-mediated degradation of the multicopper oxidase hephaestin. *J. Biol. Chem.* 279, 25696–25702.
- Ohgami, R.S., Campagna, D.R., Greer, E.L., Antiochos, B., McDonald, A., Chen, J., Sharp, J.J., Fujiwara, Y., Barker, J.E., and Fleming, M.D. (2005). Identification of a ferriductase required for efficient transferrin-dependent iron uptake in erythroid cells. *Nat. Genet.* 37, 1264–1269.
- Ohgami, R.S., Campagna, D.R., McDonald, A., and Fleming, M.D. (2006). The Steap proteins are metallo-reductases. *Blood*, in press.
- Peña, M.M.O., Lee, J., and Thiele, D.J. (1999). A delicate balance: Homeostatic control of copper uptake and distribution. *J. Nutr.* 129, 1251–1260.
- Perreault, N., and Beaulieu, J.F. (1998). Primary cultures of fully differentiated and pure human intestinal epithelial cells. *Exp. Cell Res.* 245, 34–42.
- Petris, M.J., Smith, K., Lee, J., and Thiele, D.J. (2003). Copper-stimulated endocytosis and degradation of the human copper transporter, hCtr1. *J. Biol. Chem.* 278, 9639–9646.
- Prohaska, J.R. (2000). Long-term functional consequences of malnutrition during brain development: Copper. *Nutrition* 8, 502–504.
- Prohaska, J.R., and Brokate, B. (2002). The timing of perinatal copper deficiency in mice influences offspring survival. *J. Nutr.* 132, 3142–3145.
- Prohaska, J.R., Geissler, J., Brokate, B., and Broderius, M. (2003). Copper, zinc-superoxide dismutase protein but not mRNA is lower in copper-deficient mice and mice lacking the copper chaperone for superoxide dismutase. *Exp. Biol. Med.* 228, 959–966.
- Puig, S., and Thiele, D.J. (2002). Molecular mechanisms of copper uptake and distribution. *Curr. Opin. Chem. Biol.* 6, 171–180.

- Puig, S., Lee, J., Lau, M., and Thiele, D.J. (2002). Biochemical and genetic analysis of yeast and human high affinity copper transporters suggest a conserved mechanism for copper uptake. *J. Biol. Chem.* 277, 26021–26030.
- Rae, T.D., Schmidt, P.J., Pufahl, R.A., Culotta, V.C., and O'Halloran, T.V. (1999). Undetectable intracellular free copper: The requirement of a copper chaperone for superoxide dismutase. *Science* 284, 805–808.
- Sato, M., and Gitlin, J.D. (1991). Mechanisms of copper incorporation during the biosynthesis of human ceruloplasmin. *J. Biol. Chem.* 266, 5128–5134.
- Sauer, B. (1998). Inducible gene targeting in mice using the Cre/lox system. *Methods* 14, 381–392.
- Schmidt, P.J., Kunst, C., and Culotta, V.C. (2000). Copper activation of superoxide dismutase 1 (SOD1) *in vivo*. *J. Biol. Chem.* 275, 33771–33776.
- Shim, H., and Harris, Z.L. (2003). Genetic defects in copper metabolism. *J. Nutr.* 133, 1527–1531.
- Turnlund, J.R. (1998). Human whole-body copper metabolism. *Am. J. Clin. Nutr.* 67, 960–964.
- Uauy, R., Olivares, M., and Gonzalez, M. (1998). Essentiality of copper in humans. *Am. J. Clin. Nutr.* 67, 952–959.
- Vulpe, C.D., Kuo, Y.M., Murphy, T.L., Cowley, L., Askwith, C., Libina, N., Gitschier, J., and Anderson, G.J. (1999). Hephaestin, a ceruloplasmin homologue implicated in intestinal iron transport, is defective in the *s/a* mouse. *Nat. Genet.* 21, 195–199.
- Waggoner, D.J., Bartnikas, T.B., and Gitlin, J.D. (1999). The role of copper in neurodegenerative disease. *Neurobiol. Dis.* 6, 221–230.
- West, E.C., and Prohaska, J.R. (2004). Cu,Zn-Superoxide dismutase is lower and copper chaperone CCS is higher in erythrocytes of copper-deficient rats and mice. *Exp. Biol. Med.* 229, 756–764.
- Wong, P.C., Waggoner, D., Subramaniam, J.R., Tessarollo, L., Bartnikas, T.B., Culotta, V.C., Price, D.L., Rothstein, J., and Gitlin, J.D. (2000). Copper chaperone for superoxide dismutase is essential to activate mammalian Cu/Zn superoxide dismutase. *Proc. Natl. Acad. Sci. USA* 97, 2886–2891.
- Zhang, A.-S., Xiong, S., Tuskamoto, H., and Enns, C.A. (2004). Localization of iron metabolism-related mRNAs in rat liver indicate HFE is expressed predominantly in hepatocytes. *Blood* 103, 1509–1514.